A. S. Cruces et alii, Frattura ed Integrità Strutturale, 41 (2017) 54-61; DOI: 10.3221/IGF-ESIS.41.08

Focused on Multiaxial Fatigue

Evaluation of new multiaxial damage parameters on low carbon steel

A. S. Cruces, P. Lopez-Crespo, B. Moreno
Department of Civil and Materials Engineering, University of Malaga, C/Dr Ortiz Ramos s/n, 29071 Malaga, Spain
plopezcrespo@uma.es

A. Lopez-Moreno
Department of Materials Science and Metallurgy Engineering, University of Jaen, Campus Las Lagunillas, 23071 Jaen, Spain

S. Suman
Research Center, Environmental Solution Group, Dover Corporation, Fort Payne, AL, 35967, USA

ABSTRACT. Most mechanical components are subjected to the complex fatigue loading conditions, where both amplitude and direction of loading cycles change over the time. The estimation of damage caused by these complex loading scenarios are often done by simplified uniaxial fatigue theories, which ultimately leads to higher factor of safety during the final design considerations. Critical plane-based fatigue theories have been considered more accurate for computing the fatigue damage for multiaxial loading conditions in comparison to energy-based and equivalent stress-based theories. Two recently developed fatigue theories have been evaluated in this work for the available test data. Test data includes significant amount of biaxial load paths.

KEYWORDS. Critical plane approach; Biaxial fatigue; Fatemi-Socie damage parameter.

Citation: Cruces, A. S., Lopez-Crespo, P., Moreno, B., Lopez-Moreno, A., Suman, S., Evaluation of new multiaxial damage parameters on low carbon steel, Frattura ed Integrità Strutturale, 41 (2017) 54-61.

Received: 28.02.2017
Accepted: 15.04.2017
Published: 01.07.2017

INTRODUCTION

Over the years, the analysis of complex multiaxial fatigue loading has mainly been done with the simplified uniaxial approach. This has led to the large amount of knowledge generated in this area, both from experimental [1,2] and numerical [3,4] points of view. Advanced experiments have allowed a number of features to be characterized, including surface and bulk behavior [5,6], crack-closure mechanisms [7,8], evolution of the process zone thru the thickness [9,10], crack branching processes [11], effect of variable amplitude loads such as crack acceleration [12]

or retardation [13,14] or mixed-mode local changes in the volume [15]. However, uniaxial approach does not represent the real world scenario and computation of fatigue life thru these approach often results either in under prediction or over prediction of fatigue life for the machine component. Because of the complexities and computational cost involved with the multiaxial fatigue tests, very limited amount of fatigue data are publicly available [16].
Among several other fatigue models, critical plane-based fatigue models provide more accurate prediction of fatigue lives. Critical plane-based fatigue models are based upon the determination of the location of fatigue crack initiation and microcrack –propagation [17]. The damage is computed at the plane where crack initiates, and this plane is called critical plane, however; the definition of critical plane is still controversial among the fatigue researchers. Some researchers define this plane as the plane of maximum fatigue damage, whereas other group of researchers believe that considering the plane of maximum shear stress as critical plane will be more logical and computationally cheaper.
Fatigue data from the multiaxial test on St52-3N steel specimen have been analyzed in this paper by using new Fatemi-Socie model [18] and Suman-Kallmeyer model [19]. It is well known fact that the shear stresses at the critical plane provokes the fatigue crack initiation whereas, presence of tensile stress in combination of shear stress creates condition for the microcrack to propagate. Both of the damage parameters [18,19] discussed in this paper consider the interaction of normal and shear stress at the critical plane. Both of these damage parameters [18,19] have been used to predict the fatigue life of the test specimen, and the correlation between experimental and predicted fatigue life has been analyzed.

MATERIALS AND METHODS

Material and test data have been taken from the previous biaxial fatigue test program at the University of Malaga [20]. The material that has been considered for this paper is St52-3N. The chemical composition for this steel is: 0.17% C, 1.235% Mn, 0.225% Si, 0.010% P, 0.0006% S, 0.032% Al, 0.072% Cr, 0.058% Ni and 0.016% Mo. This is a low carbon steel, and has been widely used in the structural applications in the construction, manufacturing, ship building and offshore industries [21] that combines good fatigue resistance with low environmental impact for applications where no energy is consumed during the use phase of the component [22]. Monotonic tension, compression and torsion tests were conducted to evaluate the monotonic properties of the St52-3N steel (Tab. 1). Tension tests were conducted on the solid specimens, whereas, compression and torsion tests were conducted on the tubular specimens [23]. Fig 1 shows the geometry and dimensions of the tubular specimen.

Yield stress, σ_y	386 MPa
Ultimate tensile stress, σ_u	639 MPa
Young's modulus, E	206 GPa
Shear modulus, G	78 GPa
Critical buckling stress, σ_{cr}	348 MPa

Table 1: Monotonic properties of St52-3N steel.

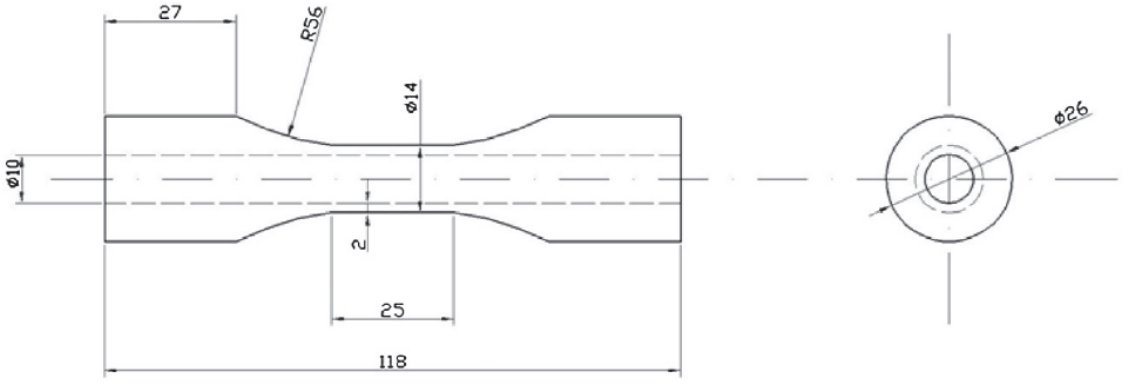

Figure 1: Geometry of the tubular hollow specimen used in the experiments. All dimensions are in mm.

The cyclic elastic-plastic material properties were obtained from the cyclic uniaxial tests. The properties obtained from the cyclic uniaxial tests have been listed in Tab. 2 & Tab. 3. ASTM standard was followed to conduct these tests.

Cyclic strength coefficient, K'	630.6 MPa
Cyclic hardening exponent, n'	0.10850
Cyclic yield strength, σ'_y	321.3 MPa
Fatigue strength coefficient, σ'_f	564.4 MPa
Fatigue strength exponent, b	-0.0576
Fatigue ductility coefficient, ε'_f	0.1554
Fatigue ductility exponent, c	-0.4658

Table 2: Monotonic properties of St52-3N steel.

Cyclic strength coefficient, K'_γ	593.8 MPa
Cyclic hardening exponent, n'_γ	0.1553
Cyclic yield strength, τ'_y	594.2 MPa
Fatigue strength coefficient, τ'_f	486.9 MPa
Fatigue strength exponent, b_γ	-0.0668
Fatigue ductility coefficient, γ'_f	0.0662
Fatigue ductility exponent, c_γ	-0.3191

Table 3: Torsional properties of St52-3N steel.

Biaxial tests require both torsional and longitudinal extensometer. It also needs a technician with good skill to place four pins of these devices [24]. As per the ASTM, load was also recommended to be applied at relatively low frequency (normally less than 4 Hz) because the weak connection between extensometer pins and the sample is preserved.
A series of in-phase biaxial tests were conducted with the strain levels that were chosen with an intension to fail the samples between 10^4 and 10^6. The design of these bi-axial fatigue tests was done on the basis of the previous uniaxial test results. Tab. 4 shows the applied axial strain amplitudes (ε_a), and shear strain amplitudes (γ_a) data for these tests. The corresponding axial stress amplitudes (σ_a) and shear stress amplitudes (τ_a) are also shown in Tab. 4 with corresponding fatigue life. Total of 13 samples were tested for this test program. All the load path for these bi-axial tests were kept proportional (Tab. 4).

CRITICAL PLANE APPROACHES

Fatemi-Socie damage parameter II (FSDP-II)

Fatemi-Socie has recently modified their earlier developed fatigue model [25]. The previous Fatemi-Socie model was based on the concept that the range of shear strain is primary reason to initiate the fatigue crack and the tensile normal stress creates secondary effects of opening the crack face. Fatemi-Socie also introduced the normal stress component to account for the rotation of principle plane axis at the critical plane. Fatemi-Socie have recently modified their damage parameter and introduced a shear stress range term to account for the interaction of normal and shear stress at the critical plane. Fatemi & Socie model resorts on the ratio of maximum normal stress and the range of shear stress to model the interaction. A material dependent parameter k has also been introduced in the parameter. Modified Fatemi-Socie fatigue damage parameter has been shown in Eq. 1 [18].

$$\frac{\Delta\gamma_{max}}{2}\left(1+k\frac{\sigma_{n,max}}{\Delta\tau}\right)=\frac{\tau'_f}{G}\left(2N_f\right)^{b\gamma}+\gamma'_f\left(2N_f\right)^{c\gamma} \quad (1)$$

$$k=\left[\frac{\frac{\tau_f'}{G}\left(2N_f\right)^{b_\gamma}+\gamma_f'\left(2N_f\right)^{c_\gamma}}{\left(1+\upsilon_e\right)\frac{\sigma_f'}{E}\left(2N_f\right)^{b}+\left(1+\upsilon_p\right)\epsilon_f'\left(2N_f\right)^{c}}-1\right]\frac{\sigma_y'}{\sigma_f'\left(2N_f\right)^{b}} \quad (2)$$

Sample	ε_a	γ_a	σ_a (MPa)	τ_a (MPa)	N_f
IP1	0.0015	0.0032	198	156	36,147
IP2	0.0015	0.0028	238	151	141,938
IP3	0.0015	0.0028	234	151	103,138
IP4	0.0015	0.0026	238	148	162,119
IP5	0.0011	0.0032	177	176	179,628
IP6	0.0011	0.0032	180	185	72,011
IP7	0.0011	0.0028	183	165	179,446
IP8	0.0011	0.0028	178	163	268,051
IP9	0.0011	0.0026	185	154	662,706
IP10	0.0009	0.0032	146	184	248,009
IP11	0.0009	0.0032	143	183	188,219
IP12	0.0009	0.0028	151	172	624,521
IP13	0.0009	0.0026	152	162	870,886

Table 4: Strain and stress conditions for in-phase strain conditions and the obtained fatigue life in number of cycles.

Suman & Kallmeyer damage parameter (SKDP)

The importance of interaction of normal and shear stress on the critical plane has recently been investigated by Suman & Kallmeyer [19]. They have used the product of normal and shear stress at the critical plane to model this interaction. The product term in Suman & Kallmeyer model represents the maximum value of the product of normal and shear stress at the critical plane. By considering this product term, Suman & Kallmeyer were able to overcome the ambiguity caused by the non-proportional loading where both normal and shear stress peaks do not occur at the same time point. This product term can model the interaction effects for wide range of in-phase and out of phase fatigue data. Apart from that, this formulation (Eq 3) also has significantly less number of material dependent parameter in comparison to the model previously developed by the same group of researchers, and provides excellent correlation between experimental and predicted fatigue lives of the steel and titanium specimen. Suman & Kallmeyer fatigue model also captures the effect of strain hardening due to LCF loading and the mean shear stress at the critical plane.

$$DP=\left(G\cdot\Delta\gamma\right)^{w}\cdot\tau_{max}^{(1-w)}\cdot\left(1+k\frac{\left(\sigma\cdot\tau\right)_{max}}{\sigma_0^2}\right) \quad (3)$$

RESULTS

In this study, most of the load path used are proportional and sinusoidal. Due to the proportionality, both shear and normal stress peaks in these tests happened at the same time point. The critical plane stresses for the test IP1 (Tab. 4) are presented in Fig 2 and Fig 4. The peaks of normal and shear stresses are presented by solid and dashed lines respectively, and the damage parameter values are presented by the green solid line (damage parameter is obtained with the maximum load).

Fatemi-Socie damage parameter II

It can be observed from the plots in Fig 2 that the maximum value of Fatemi-Socie damage parameter and the maximum value for shear stress range is not at the same time point, which implies that the plane of maximum shear and plane of maximum damage parameter is far apart.

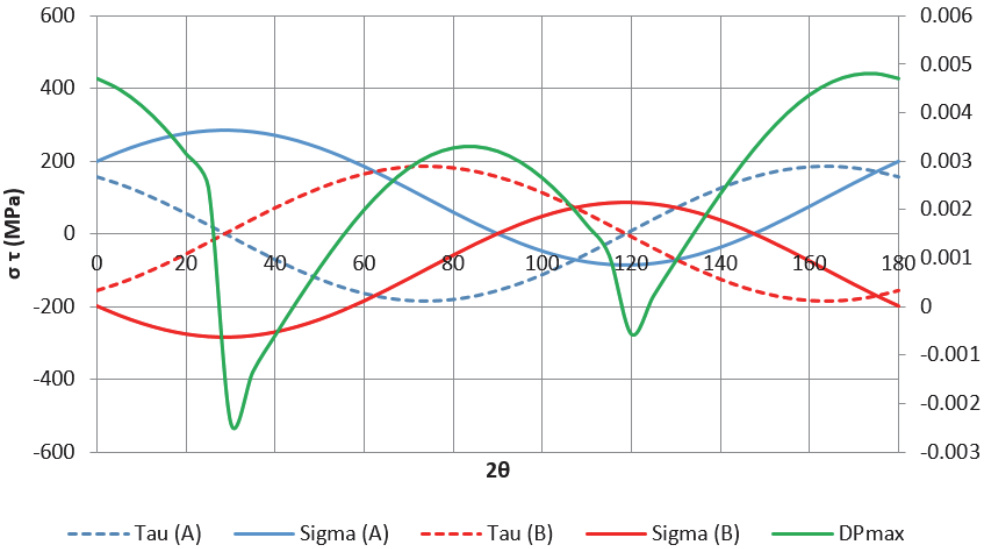

Figure 2: IP 1 – σ, τ and FSDP-II at max peak cycle (A) and min peak cycle (B).

FSDP-II was computed for all the test data shown in Tab. 4, and the damage parameter value was presented against the cycles to failure. The plot is shown in Fig 3, and it can be noticed that the FSDP-II models most of the LCF fatigue behavior data but it produces significant scatter in the HCF data range.

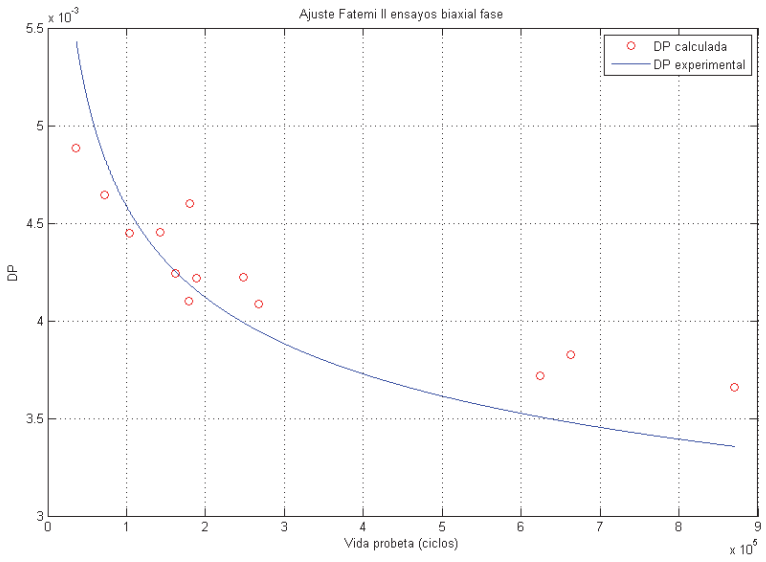

Figure 3: Fatigue life correlation for St52-3N steel based on Fatemi II model

Suman-Kallmeyer Damage parameter

In contrast to Fatemi-Socie damage parameter, the difference in the location of maximum shear stress range plane and the plane where the value of Suman & Kallmeyer damage parameter value is maximum is much smaller. While computing the damage parameter for the proportional load path, computation of maximum shear plane was comparatively easy.

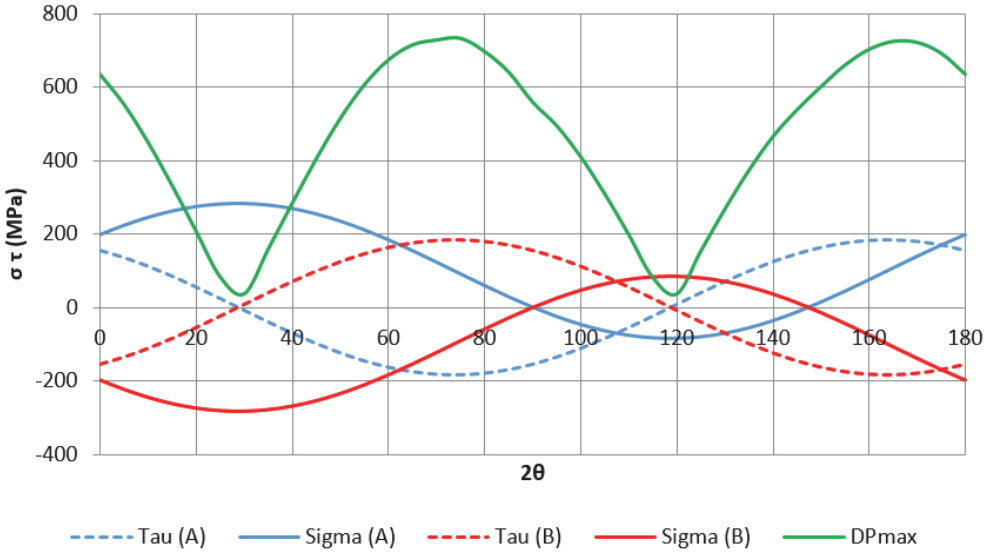

Figure 4: IP 1 – σ, τ and SKDP at max peak cycle (A) and min peak cycle (B)

SKDP was computed for the test data shown in Tab. 4, and the material dependent parameters were optimized with a dual power law fit line. After several iterations of computations to optimize these damage parameter, it was observed that fit was good for larger w & k values for this data set. The direction of shear stress in this parameter is not taken into the account because both positive and negative shear stress create same crack initiation phenomenon.
The damage parameter vs cycles to failure for the Suman-Kallmeyer damage parameter is shown in fig 5, and it can be observed from the curve that both LCF and HCF data have collapsed very well along the fitting line. Comparison of fig 3 and fig 5 appears to indicate that the Suman-Kallmeyer damage parameter provided better correlation for the test data.

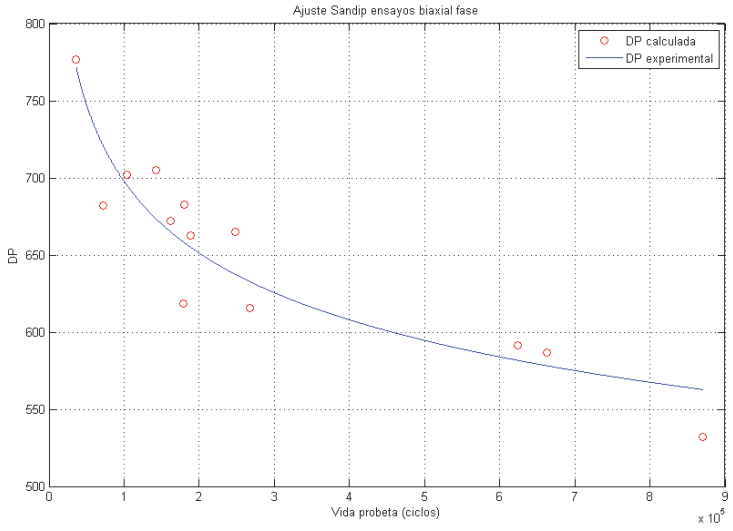

Figure 5: Fatigue life correlation for St52-3N steel based on Sandip model (k=2.1, w=1.1).

Life-Life plots were also created for the test data by using both Fatemi-Socie II [18] damage parameter and the damage parameter proposed by Suman-Kallmeyer [19]. Red square in fig 6 represent the life predicted by FSDP II, and green triangles represent the life predicted by SKDM model. By observing this plot (fig 6) and the data, the FSDP II tends to overestimate the fatigue life and the SKDP tends to underestimate the fatigue life. Similar level of correlation is observed on both damage parameters. The two new theories give overall good predictions for the test data under study.

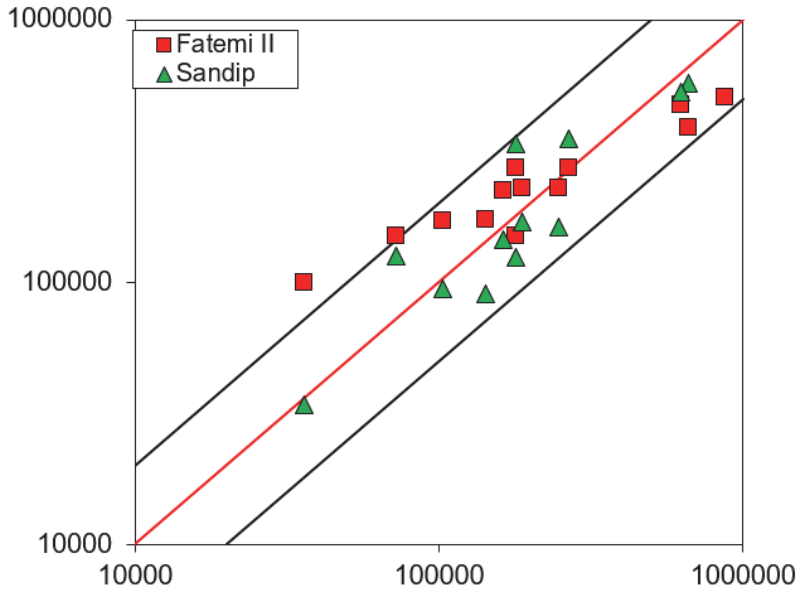

Figure 6: Predicted vs. experimental life for St52-3N using Fatemi II model and Sandip model.

Conclusion

Two recently developed fatigue theories have been studied on experimental data. The experimental data were acquired on biaxial tests combining tension-compression and torsion under proportional load. The two fatigue theories were based on the critical plane approach. One of them is an enhanced formulation of the Fatemi-Socie damage parameter. The other theory uses the product of the normal and the shear stress at the critical plane. Both theories provided an overall good prediction for the loading cases analyzed. While the new Fatemi-Socie damage parameter tended to overestimate the fatigue life preditions, the Suman-Kallmeyer tended to underestimate the life preditions.

Acknowledgements

Authors would like to acknowledge financial support of Junta de Andalucía thru Proyectos de Excelencia grant reference TEP-3244, Campus de Excelencia Internacional del Mar (CEIMAR) and Ministerio de Economía y Competitividad thru grant reference MAT2016-76951-C2-2-P.

References

[1] Christopher CJ, Lu Y, Patterson EA. Local crack plasticity and its influences on the global elastic stress field. Int J Fatigue 2013;46:4–15.

[2] Zanganeh M, Lopez-Crespo P, Tai YH, Yates JR. Locating the crack tip using displacement field data: a comparative study. Strain 2013;49:102–15.

[3] Branco R, Antunes FV. Finite element modelling and analysis of crack shape evolution in mode-I fatigue Middle Cracked Tension specimens. Eng Fract Mech 2008;75:3020–37. doi:10.1016/j.engfracmech.2007.12.012.

[4] Lopez-Crespo P, Pommier S. Numerical analysis of crack tip plasticity and history effects under mixed mode conditions. J Solid Mech Mater Eng 2008;2:1567–76.

[5] Rodopoulos CA. Fatigue Damage from Surface to Bulk. In: Sih GC, editor. Multiscale Fatigue Crack Initiat. Propag. Eng. Mater. Struct. Integr. Microstruct. Worthiness Fatigue Crack Growth Behav. Small Large Bodies, Dordrecht: Springer Netherlands; 2008, p. 113–31. doi:10.1007/978-1-4020-8520-8_6.

[6] Lopez-Crespo P, Mostafavi M, Steuwer A, Kelleher JF, Buslaps T, Withers PJ. Characterisation of overloads in fatigue by 2D strain mapping at the surface and in the bulk. Fatigue Fract Eng Mater Struct 2016;39:1040–8.
[7] Pippan R, Grosinger W. Fatigue crack closure: From LCF to small scale yielding. Int J Fatigue 2013;46:41–8.
[8] Pippan R, Hohenwarter A. Fatigue crack closure: a review of the physical phenomena. Fatigue Fract Eng Mater Struct 2017;40:471–95. doi:10.1111/ffe.12578.
[9] Skorupa M, Skorupa A, Schijve J, Machniewicz T, Korbut P. Effect of specimen thickness and stress ratio on fatigue crack growth after a single overload cycle on structural steel. Eur. Conf. Fract. ECF 13, San Sebastian: 2000.
[10] Camas D, Lopez-Crespo P, Gonzalez-Herrera A, Moreno B. Numerical and experimental study of the plastic zone in cracked specimens. Eng Fract Mech 2017. doi:10.1016/j.engfracmech.2017.02.016.
[11] Lu S, Bao R, Zhang T, Fei B. A link-up resulted fatigue crack branching in Al–Cu–Mg alloy. Int J Fatigue 2016;92:459–69. doi:10.1016/j.ijfatigue.2016.02.036.
[12] Zitounis V, Irving P. Fatigue crack acceleration effects during tensile underloads in 7010 and 8090 aluminium alloys. Int J Fatigue 2007;29:108–18. doi:10.1016/j.ijfatigue.2006.02.048.
[13] Lopez-Crespo P, Steuwer A, Buslaps T, Tai YH, Lopez-Moreno A, Yates JR, et al. Measuring overload effects during fatigue crack growth in bainitic steel by synchrotron X-ray diffraction. Int J Fatigue 2015;71:11–6.
[14] Salvati E, O'Connor S, Sui T, Nowell D, Korsunsky AM. A study of overload effect on fatigue crack propagation using EBSD, FIB–DIC and FEM methods. Eng Fract Mech 2016;167:210–23. doi:10.1016/j.engfracmech.2016.04.034.
[15] Toda H, Sinclair I, Buffière J-Y, Maire E, Khor KH, Gregson P, et al. A 3D measurement procedure for internal local crack driving forces via synchrotron X-ray microtomography. Acta Mater 2004;52:1305–17. doi:10.1016/j.actamat.2003.11.014.
[16] Wang YY, Yao WX. Evaluation and comparison of several multiaxial fatigue criteria. Int J Fatigue 2004;26:17–25.
[17] Socie DF, Marquis GB. Multiaxial Fatigue. Warrendale, PA (USA): Society of Automotive Engineers, Inc.; 2000.
[18] Gates NR, Fatemi A. Interaction of shear and normal stresses in multiaxial fatigue damage analysis. Frat Ed Integrità Strutt 2016;37:160–5. doi:10.3221/IGF-ESIS.37.22.
[19] Suman S, Kallmeyer A, J S. Development of a multiaxial fatigue damage parameter and life prediction methodology for non-proportional loading. Frat Ed Integrità Strutt 2016;38:224–30. doi:10.3221/IGF-ESIS.38.30.
[20] Lopez-Crespo P, Garcia-Gonzalez A, Moreno B, Lopez-Moreno A, Zapatero J. Some observations on short fatigue cracks under biaxial fatigue. Theor Appl Fract Mech 2015;80:96–103.
[21] Mokhtarishirazabad M, Lopez-Crespo P, Moreno B, Lopez-Moreno A, Zanganeh M. Optical and analytical investigation of overloads in biaxial fatigue cracks. Int J Fatigue 2017. doi:10.1016/j.ijfatigue.2016.12.035.
[22] Chaves V. Ecological criteria for the selection of materials in fatigue. Fatigue Fract Eng Mater Struct 2014;37:1034–42. doi:10.1111/ffe.12181.
[23] Lopez-Crespo P, Moreno B, Lopez-Moreno A, Zapatero J. Study of crack orientation and fatigue life prediction in biaxial fatigue with critical plane models. Eng Fract Mech 2015;136:115–30.
[24] Lopez-Crespo P, Moreno B, Lopez-Moreno A, Zapatero J. Characterisation of crack-tip fields in biaxial fatigue based on high-magnification image correlation and electro-spray technique. Int J Fatigue 2015;71:17–25.
[25] Fatemi A, Socie DF. A Critical Plane approach to multiaxial fatigue damage including out-of-phase loading. Fatigue Fract Eng Mater Struct 1988;11:149–65.